2016 American Control Conference (ACC)
Boston Marriott Copley Place
July 6-8, 2016. Boston, MA, USA

Experimental Investigation of Spatial Spillover in Adaptive Feedback Noise Control of Broadband Disturbances in a 3D Acoustic Space

Antai Xie[1] and Dennis S. Bernstein[2]

Abstract— **Active feedback noise control for rejecting broadband disturbances must contend with the Bode integral constraint, which implies that suppression over some frequency range gives rise to amplification over another range. This is called *spectral spillover*. In the present paper, we apply retrospective cost adaptive control (RCAC) to active noise suppression in the interior of an automobile. This study highlights spectral spillover along with related issues, such as the need for controller stability, the effect of plant rolloff at DC, and the challenge of nonminimum-phase zeros. Beyond these issues, this paper deals with *spatial spillover*, which refers to the amplification of noise at locations where no microphone is located. Typically, this issue is dealt with by restricting the bandwidth to a frequency range within which the acoustic wavelength is sufficiently large such that the phase shift between sensor locations is minimal. However, in this study we show that this design guideline is not valid in the case where obstructions (such as the driver of the vehicle) are present. This study illuminates the interaction among modeling and hardware issues within the context of a real-world application. At the same time, it provides a case study illustrating RCAC and its performance and requirements in practice.**

I. Introduction

Active noise suppression has been extensively studied for several decades, and numerous techniques have been developed, analyzed, and tested, with several highly successful applications [1–3]. Roughly speaking, noise suppression algorithms can be classified as either feedforward or feedback. Feedforward algorithms assume that a direct or indirect measurement of the disturbance is available, and this signal is passed through an adaptive filter to a control speaker [2, 3]. These algorithms assume that the disturbance measurement is not corrupted by the control speaker output, which means that the transfer function from the control input to the disturbance measurement is zero. Consequently, the only feedback in the system is the adaptation loop, which typically operates at a much slower rate than the time constant of the acoustics. The absence of a fast feedback loop means that these algorithms are less susceptible to instability.

In some applications, however, it is difficult to measure the disturbance either directly or indirectly. For example, in the case of interior noise in a ground vehicle, it is difficult for external sensors to measure the effect of road and wind noise on the interior of the vehicle. If, however, internal microphones are used, then the measurements include the effect of the control speakers. In this situation, feedback control is a more appropriate architecture than feedforward control. However, feedback control is more challenging to implement due to its greater susceptibility to instability in the event of model errors.

Aside from the requirement in feedforward control that the disturbance measurement be uncorrupted by the control input and the fact that instability can occur in feedback control, these techniques differ in their performance relative to the disturbance spectrum. Both techniques perform well in the presence of narrowband (for example, tonal) disturbances [3, 4]. However, suppressing broadband disturbances is challenging for both methods. An overall limiting causality constraint exists in broadband feedforward control, where a delay in the transfer function from the control input to the performance microphone must be compensated for by a delay of at least equal length in the transfer function from the disturbance to the performance microphone [3, p. 60].

Although feedback control can suppress broadband noise, two caveats must be addressed. First, the Bode integral constraint implies that reducing the magnitude of the frequency response is impossible at all frequencies [5–7]. For narrowband disturbances, this does not present a problem since the noise spectrum is confined to a limited bandwidth. However, for broadband disturbances, it is inevitable that, at least in some frequency range, the closed-loop noise level is amplified relative to the open-loop noise level. The challenge is thus to shape the closed-loop response so that *spectral spillover* has minimal effect on the closed-loop performance. In active noise control this is especially challenging due to the A-weighting effect of human hearing, which emphasizes the high frequency range. The second caveat relating to broadband noise suppression is the fact that many adaptive feedback control algorithms focus on model-reference architectures [8, 9]. Consequently, feedback control for broadband disturbance rejection remains a challenging problem within the context of adaptive noise control.

Beyond the problem of spectral spillover, yet another challenge is the presence of *spatial spillover*. This refers to the phenomenon that noise suppression at one location may give rise to noise amplification at another location. In an infinite acoustic space without obstructions, this effect can be determined in terms of the phase shift of an acoustic wave as a function of frequency and distance; the phase shift determines the amplification relative to perfect cancellation due to the superposition of two acoustic waves. Figure 1 shows how cancellation transitions to amplification as a function of phase shift.

Unfortunately, in applications involving an enclosed space,

[1]Graduate Student at the Department of Aerospace Engineering, University of Michigan, 1320 Beal Ave., Ann Arbor, MI 48109
[2]Professor at the Department of Aerospace Engineering, University of Michigan, 1320 Beal Ave., Ann Arbor, MI 48109

such as the interior of a vehicle, the phase shift between two points is no longer a simple function of frequency and distance, but instead depends on reflections and obstructions within the acoustic space.

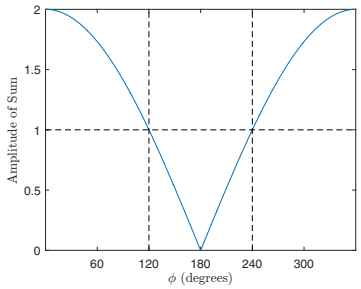

Fig. 1. Amplitude of the sum of two superposed unit-amplitude sinusoids with relative phase ϕ. For $\phi = 180°$, the amplitude of the sum is zero. For $\phi = 180° \pm 60°$, the amplitude of the sum is 1. The plot is based on the fact that $\sin(\omega t) + \sin(\omega t + \phi) = 2\cos(\phi/2)\sin(\omega t + \phi/2)$.

To this end, the goal of the present paper is to investigate the effect of spatial spillover within a finite 3D acoustic space. To do this, we apply retrospective cost adaptive control (RCAC) to active noise suppression for broadband disturbances in the interior of an automobile. In particular, we measure the acoustic suppression at multiple points within the vehicle, and we measure the relative phase shift as well as the noise level. RCAC was originally developed in [10], where both tonal and broadband noise were considered in acoustic duct experiments. This technique was further developed in [11–13]. In [14], RCAC was applied in simulation to structural vibration suppression with broadband disturbances.

The purpose of this paper is to present the results of an experimental application of RCAC to broadband disturbance rejection. In particular, the goal is to assess the ability of RCAC to suppress the effects of broadband disturbances in a vehicle interior under limited modeling information about the geometry of the vehicle. These experiments involve static (non-driving) tests, where the disturbances are provided by speakers, and microphones and speakers are used for feedback control.

The contents of the paper are as follows. Section II describes the experimental setup. In Section III, experimental results of RCAC in static testing are presented. An analysis of spatial spillover with examples is discussed in Section IV. Section V shows the effect of an obstruction on the relative phase of two microphones. Conclusions are presented in Section VI.

II. Experimental Setup

We use Real Time Workshop (RTW) in the MATLAB/Simulink environment with a dSPACE DS1005 Autobox in order to implement RCAC in the vehicle. A DS2004 I/O board and DS2102 I/O board are used for A/D and D/A conversions. Acoustic sensing is provided by omnidirectional microphones with rated bandwidth from 50 Hz to 16 kHz. Acoustic actuation is provided by car audio speakers mounted on the vehicle doors. Additional hardware includes car speaker amplifiers, microphone amplifiers, and analog filters to avoid aliasing.

We consider only SISO feedback control where the controlled plant is from a single speaker to a single microphone. Two evaluation microphones are placed on the driver seat headrest to evaluate qualitative cancellation for a person in the driver seat. We denote the left headrest as LH and the right headrest as RH. We consider five locations, p_1, p_2, p_3, RH, and LH, to place the z microphone. Four door speakers are available as either the control speaker or to provide the disturbance. We denote these by front driver speaker FDS, front passenger speaker FPS, rear driver speaker RDS, and rear passenger speaker RPS. Figure 2 shows the approximate locations of the microphones and speakers in the vehicle.

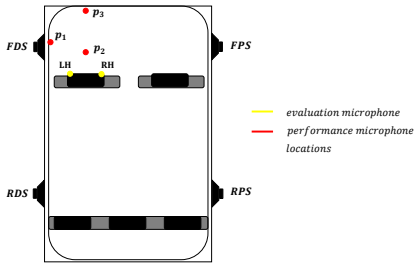

Fig. 2. Vehicle microphone and speaker placement.

III. Experimental Results

In this section we present results of static vehicle tests, that is, with the vehicle parked and the disturbance provided by one of the speakers. We perform all tests with a person sitting in the driver seat. The controlled plant is from a single control speaker to a single performance microphone. A separate speaker is used to provide the disturbance. In all cases, we consider a broadband disturbance profile with two resonance peaks centered at 140 Hz and 200 Hz. This is consistent with a typical road noise spectrum. The frequency range of interest for this application is from 50 Hz to 300 Hz and all data is sampled at 1 kHz. All frequency-domain data is A-weighted with 1-Hz resolution. We evaluate the noise reduction between the open-loop and closed-loop systems at the performance and evaluation microphones after RCAC converges.

Choice of RCAC target model G_{f}. It is known that if a zero of G_{zu} is not modeled in G_{f}, then RCAC may place a controller pole at the location of the zero [15]. In order to avoid non-asymptotically stable pole-zero cancellation, we model all NMP zeros (including zeros on the unit-circle) of G_{zu} in G_{f}.

In order to experimentally identify the NMP zeros of G_{zu}, we take advantage of the fact that RCAC may place controller poles at unmodeled zeros by choosing $G_{\mathrm{f}}(\mathbf{z}) = \frac{1}{\mathbf{z}}$. We then allow unstable pole-zero cancellation between G_{c} and G_{zu} and then check the poles of the controller just before the system diverges in order to obtain estimates of the locations of the NMP zeros. It was found that, for all z locations that were considered, including NMP zeros at 1.15 and 2.37 in G_{f} produced stabilizing controllers with proper tuning. The fact that these NMP zeros are fixed for different z locations suggests that these zeros are not due to

the acoustics, but rather are due to electrical or mechanical hardware in the loop.

We note that G_{zu} has zeros on the unit circle at 1 due to the zero DC response of the acoustics and the electronics. In order to prevent non-asymptotically stable pole-zero cancellation at DC, we model two zeros at 1 in G_{f}, one to represent the zero DC response of the control speaker and one to represent the zero DC response of the z microphone.

The target model G_{f} is chosen to be

$$G_{\mathrm{f}}(\mathbf{z}) = \frac{H_d(\mathbf{z}-1)^2(\mathbf{z}-1.15)(\mathbf{z}-2.37)}{\mathbf{z}^{4+d}}, \qquad (1)$$

where d is the relative degree of G_{zu} and H_d of G_{zu} is an approximation of the first nonzero Markov parameter. We obtain H_d and d from the impulse response as seen in Figure 3. Note that d and H_d change with different z locations.

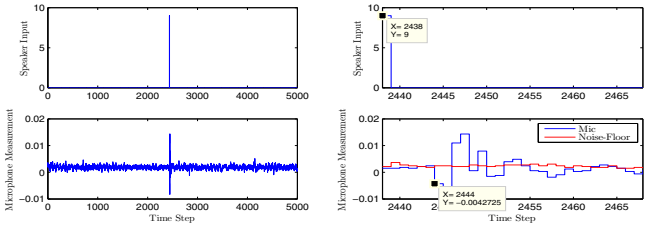

Fig. 3. The impulse response of the transfer function from FPS to z, with the z microphone placed at p_1. We use a discrete-time impulse with amplitude 9 V to minimize corruption due to sensor noise. It can be seen on the right that d is 6 and $H_d \approx -0.00427$.

Controller Stability Constraint. As shown in [16], RCAC controllers share characteristics with high-authority LQG controllers as well as pole-placement controllers. Accordingly, RCAC may converge to an unstable controller. However, experience shows that instability may occur with an unstable controller even when the closed-loop system is stable due to a combination of saturation and noise. In order to prevent RCAC from converging to an unstable controller, we implement the following technique that can be executed at the 1-kHz sample rate. After each controller update, we check

$$\sum_{i=1}^{n_c} |\theta_{\mathrm{den}}(i)| < \alpha, \qquad (2)$$

where $\alpha > 0$ and the components of θ_{den} are the coefficients of the denominator of the controller. If (2) is violated, then the controller is not updated and the controller from the previous step is used. Using this technique we can constrain the spectral radius of the controller.

Example 1: Closed-loop performance of RCAC with the z microphone placed at p_1, FPS as the control speaker, and RPS as the disturbance speaker. Figure 4 shows the closed-loop power spectral density of the performance and evaluation microphones.

Example 2: Closed-loop performance of RCAC with the z microphone placed at p_2, FPS as the control speaker, and RPS as the disturbance speaker. Figure 5 shows the closed-loop power spectral density of the performance and evaluation microphones.

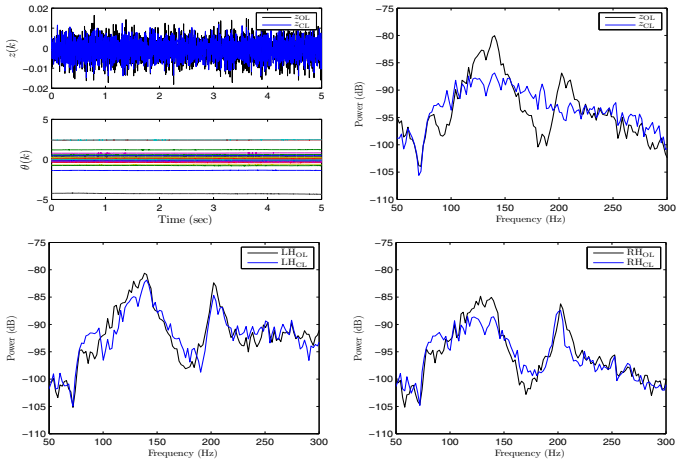

Fig. 4. Example 1: Closed-loop performance of RCAC with the z microphone placed at p_1, FPS as the control speaker, and RPS as the disturbance speaker. At z, the peak in the open-loop response centered at 140 Hz is suppressed from 115 Hz to 155 Hz in closed loop, with 6.8 dB power suppression at the center frequency 140 Hz. The peak in the open-loop response centered at 200 Hz is suppressed from 195 Hz to 220 Hz in closed loop, with 5.1 dB power suppression at the center frequency 200 Hz. At LH, suppression of the open-loop response centered at both peaks is minimal. At RH, the peak in the open-loop response centered at 140 Hz is suppressed from 115 Hz to 145 Hz in closed loop, with 3.9 dB power suppression at the center frequency 140 Hz. Suppression of the peak centered at 200 Hz is minimal.

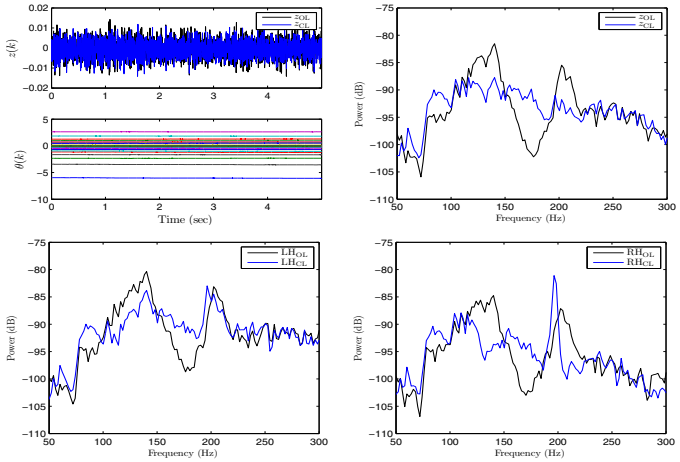

Fig. 5. Example 2: Closed-loop performance of RCAC with the z microphone placed at p_2, FPS as the control speaker, and RPS as the disturbance speaker. At z, the peak in the open-loop response centered at 140 Hz is suppressed from 110 Hz to 150 Hz in closed loop, with 6.2 dB power suppression at the center frequency 140 Hz. The peak in the open-loop response centered at 200 Hz is suppressed from 195 Hz to 220 Hz in closed loop, with 6.3 dB power suppression at the center frequency 200 Hz. Spectral spillover primarily occurs from 150 Hz to 195 Hz. At LH, the peak in the open-loop response centered at 140 Hz is suppressed from 105 Hz to 150 Hz in closed loop, with 3.5 dB power suppression at the center frequency 140 Hz. Suppression of the peak centered at 200 Hz is minimal. At RH, the peak in the open-loop response centered at 140 Hz is suppressed from 115 Hz to 150 Hz in closed loop, with 9.1 dB power suppression at the center frequency 140 Hz. The peak in the open-loop response centered at 200 Hz is suppressed from 200 Hz to 220 Hz in closed loop, with 7.1 dB power suppression at the center frequency 200 Hz. However, there is sharp amplification at 196 Hz.

IV. Spatial Spillover

In this section, we analyze the spatial spillover between the performance microphone, which is used in feedback, and the

evaluation microphones, which are not used for feedback but are used only for diagnostics. Consider the transfer function from the input u and disturbance w to the performance z and evaluation microphone e, where

$$z = G_{zu}u + G_{zw}w, \tag{3}$$

$$e = G_{eu}u + G_{ew}w, \tag{4}$$

and feedback control u is given by

$$u = G_{\rm c}z. \tag{5}$$

Thus,

$$z = \widetilde{G}_{zw}w, \tag{6}$$

where

$$\widetilde{G}_{zw} \triangleq \frac{G_{zw}}{1 - G_{zu}G_{\rm c}}. \tag{7}$$

It follows from (4), (5), and (6) that

$$e = \widetilde{G}_{ew}w, \tag{8}$$

where

$$\widetilde{G}_{ew} \triangleq G_{eu}G_{\rm c}\widetilde{G}_{zw} + G_{ew}. \tag{9}$$

Define the spatial spillover function $G_{\rm ss}$ by

$$G_{\rm ss} \triangleq \frac{\dfrac{\widetilde{G}_{ew}}{G_{ew}} - 1}{\dfrac{\widetilde{G}_{zw}}{G_{zw}} - 1}, \tag{10}$$

where

$$\frac{\widetilde{G}_{zw}}{G_{zw}} - 1 = \frac{G_{zu}G_{\rm c}}{1 - G_{zu}G_{\rm c}} \tag{11}$$

and

$$\frac{\widetilde{G}_{ew}}{G_{ew}} - 1 = \frac{G_{eu}G_{\rm c}G_{zw}}{G_{ew}(1 - G_{zu}G_{\rm c})}. \tag{12}$$

It follows from (10), (11), and (12) that

$$G_{\rm ss} = \frac{\dfrac{G_{eu}G_{\rm c}G_{zw}}{G_{ew}(1 - G_{zu}G_{\rm c})}}{\dfrac{G_{zu}G_{\rm c}}{1 - G_{zu}G_{\rm c}}} = \frac{G_{eu}G_{zw}}{G_{zu}G_{ew}}, \tag{13}$$

which shows that $G_{\rm ss}$ can be written in terms of the open-loop transfer functions G_{eu}, G_{zw}, G_{zu}, and G_{ew}. We rewrite (10) as

$$\frac{\widetilde{G}_{ew}}{G_{ew}} - 1 = \left(\frac{\widetilde{G}_{zw}}{G_{zw}} - 1\right) G_{\rm ss}. \tag{14}$$

Note that, if

$$\angle G_{\rm ss} = 0^\circ, \quad |G_{\rm ss}| = 1, \tag{15}$$

then

$$\frac{\widetilde{G}_{ew}}{G_{ew}} = \frac{\widetilde{G}_{zw}}{G_{zw}}. \tag{16}$$

If w is colocated with u or z is equal to e, then (15) is satisfied for all frequencies. Table I provides a qualitative comparison of the performance of the evaluation microphone relative to the z microphone based on $G_{\rm ss}$ and experimental observations.

TABLE I

OBSERVATIONS ON THE PERFORMANCE AND SPATIAL SPILLOVER OF THE EVALUATION MICROPHONE RELATIVE TO THE z MICROPHONE.

	$\lvert G_{\rm ss}\rvert < 0.5$	$\lvert G_{\rm ss}\rvert \approx 1$	$\lvert G_{\rm ss}\rvert > 2$
$\lvert\angle G_{\rm ss}\rvert < 10^\circ$	1. Good suppression	2. Good suppression	3. Fair suppression
$10^\circ < \lvert\angle G_{\rm ss}\rvert < 30^\circ$	4. Good suppression	5. Fair suppression	6. Limited suppression
$30^\circ < \lvert\angle G_{\rm ss}\rvert < 90^\circ$	7. Fair suppression	8. Limited suppression	9. Limited suppression
$90^\circ < \lvert\angle G_{\rm ss}\rvert$	10. Minimal Spillover	11. Some Spillover	12. Large Spillover

Next, we discuss the suppression of the primary peaks at the z, LH, and RH microphones qualitatively, and reference the cases in Table I to analyze spatial spillover. We note that some of the preceding examples will fall slightly outside the predicted trends of Table I which could possibly be a result of nonlinear effects.

Example 3: Spatial spillover at the evaluation microphones with the z microphone colocated with LH, FPS as the control speaker, and RPS as the disturbance speaker. Figure 6 shows the closed-loop power spectral density of the performance and evaluation microphones, as well as $G_{\rm ss}$ between z and the evaluation microphones.

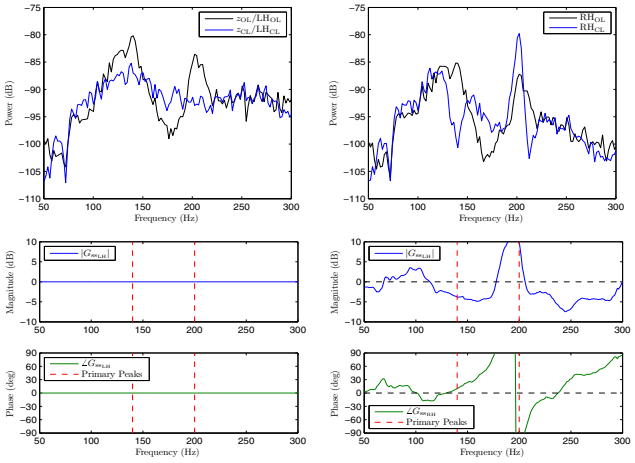

Fig. 6. Example 3: Spatial spillover at the evaluation microphones with the z microphone colocated with LH, FPS as the control speaker, and RPS as the disturbance speaker. At z/LH, both the peak centered at 140 Hz and 200 Hz are suppressed. At RH, for the peak centered at 140 Hz, cases 1, 2, and 4 apply, resulting in good suppression as expected. For the peak centered at 200 Hz, case 12 applies, resulting in sharp amplification as expected.

Example 4: Spatial spillover at the evaluation microphones with the z microphone colocated with RH, FPS as the control speaker, and RPS as the disturbance speaker. Figure 7 shows the closed-loop power spectral density of

the performance and evaluation microphones, as well as $G_{\rm ss}$ between z and the evaluation microphones.

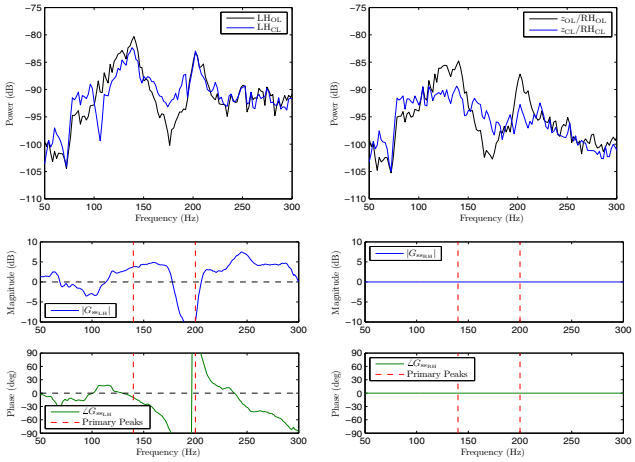

Fig. 7. Example 4: Spatial spillover at the evaluation microphones with the z microphone colocated with RH, FPS as the control speaker, and RPS as the disturbance speaker. At the z/RH microphone, both the peak centered at 140 Hz and 200 Hz are suppressed. At LH, for the peak centered at 140 Hz, case 5 applies, resulting in fair suppression as expected. For the peak centered at 200 Hz, case 10 applies. We expect to see minimal spillover, however possibly due to $|G_{\rm ss}| << 0.5$, no spillover is observed.

Example 5: Spillover at the evaluation microphones for Example 2. Figure 8 shows $G_{\rm ss}$ between z and the evaluation microphones for Example 2.

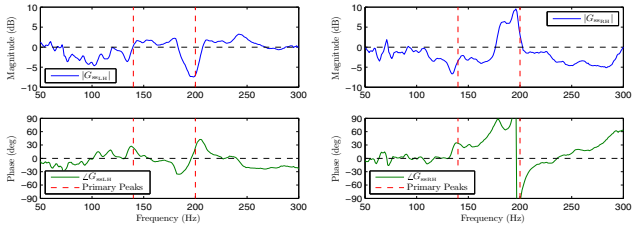

Fig. 8. Example 5: Spatial spillover at the evaluation microphones for Example 2. At LH, for the peak centered at 140 Hz, cases 2 and 5 apply, resulting in suppression as expected. For the peak centered at 200 Hz, case 7 applies. We expect to see fair suppression, however limited suppression is observed. At RH, for the peak centered at 140 Hz, cases 2 and 5 apply, resulting in suppression as expected. For the peak centered at 200 Hz, case 12 applies, resulting in sharp amplification as expected.

Example 6: Spatial spillover at the evaluation microphones with the z microphone placed at p_3, FPS *as the control speaker, and* RPS *as the disturbance speaker*. Figure 9 shows the closed-loop power spectral density of the performance and evaluation microphones, as well as $G_{\rm ss}$ between z and the evaluation microphones.

V. Obstruction in Vehicle

In this section, we examine the relative phase between the two evaluation microphones driven by u, that is $\angle(\frac{G_{{\rm LH}u}}{G_{{\rm RH}u}})$, with and without a person in the driver seat. We show that the acoustics in the interior of the vehicle within the frequency range of interest can change significantly when there is an obstruction between the sensor locations. This can effect the

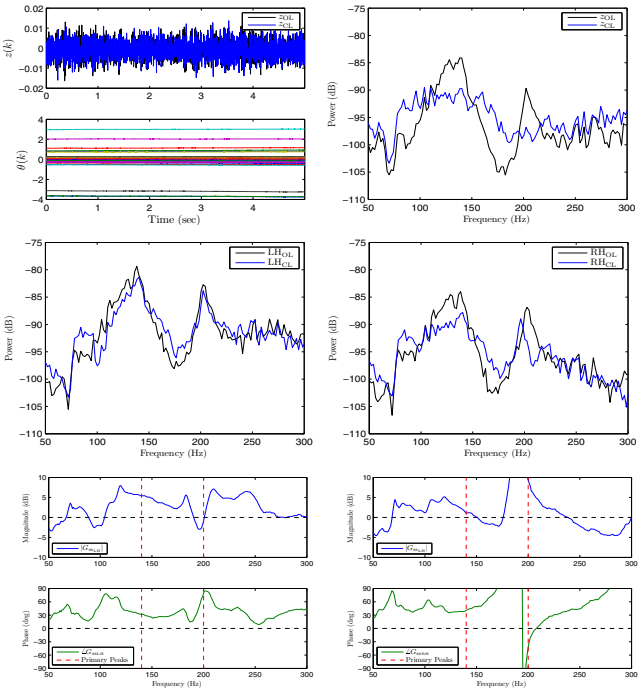

Fig. 9. Example 6: Spatial spillover at the evaluation microphones with the z microphone placed at p_3, FPS as the control speaker, and RPS as the disturbance speaker. At z, both the peak centered at 140 Hz and 200 Hz are suppressed. At LH, for the peak centered at 140 Hz, cases 6 and 9 apply, resulting in limited suppression as expected. For the peak centered at 200 Hz, case 8 applies, resulting in limited suppression as expected. At RH, for the centered peak at 140 Hz, case 8 applies. We expect to see limited suppression, however fair suppression is observed. For the peak centered at 200 Hz, cases 9 and 12 apply. We expect to see a sharp amplification, but limited spillover is observed.

performance at z as well as spatial spillover at the evaluation microphones since there is a significant shift in the acoustics.

Example 7: Comparison of the relative phase of the evaluation microphones using FDS *and* FPS *as a single input u*. Figure 10 shows the relative phase of the evaluation microphones driven by u with and without a person in the driver seat.

Example 8: Comparison of the relative phase using all four speakers as a single input u. Figure 11 shows the relative phase of the evaluation microphones driven by u with and without a person in the driver seat.

VI. Conclusions

For all locations of the performance microphone, RCAC suppressed the disturbance at the primary disturbance peaks. Therefore, due to the Bode integral constraint, spectral spillover occurs across other bands. By using additional evaluation microphones for diagnostics, we observed that, while noise was suppressed at the performance microphone, reduced suppression or, in the worst cases, sharp amplification due to spatial spillover occurred at the evaluation microphone. In the case where obstructions, such as the presence of a person in the driver seat, were present in the vehicle, we saw increased relative phase shift compared to the vehicle without a person in the driver seat. To overcome some of these issues, the next step is to implement

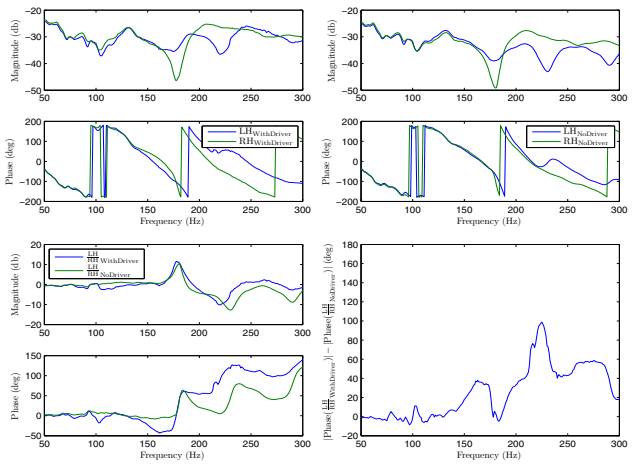

Fig. 10. Example 7: Comparison of the relative phase of the evaluation microphones with and without a person in the driver seat using FDS and FPS as a single input. Bottom left shows the frequency response of $\frac{G_{\mathrm{LH}u}}{G_{\mathrm{RH}u}}$ with and without a person in the driver seat. Bottom right shows the difference in the magnitude of the relative phase of the evaluation microphones with and without a person in the driver seat. A positive difference indicates that the relative phase shift is worse with a person in the driver seat. Below 150 Hz, the difference in relative phase is small. However, above 150 Hz, a person in the driver seat significantly increases the relative phase between the evaluation microphones.

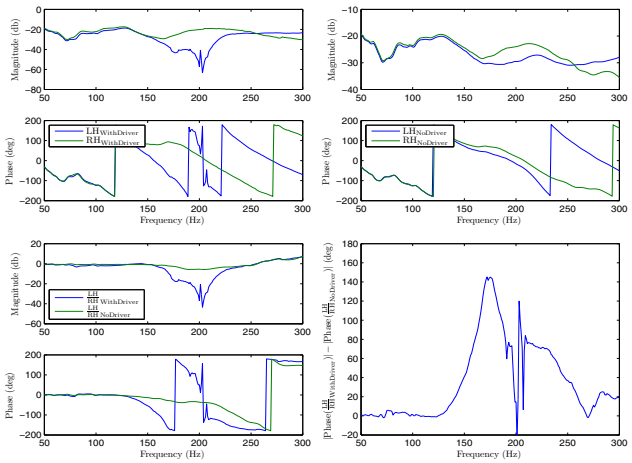

Fig. 11. Example 8: Comparison of the relative phase of the evaluation microphones with and without a person in the driver seat using all four speakers as a single input. Bottom left shows the frequency response of $\frac{G_{\mathrm{LH}u}}{G_{\mathrm{RH}u}}$ with and without a person in the driver seat. A large anti-resonance occurs at 200 Hz with a person is in the driver seat. Bottom right shows the difference in the magnitude of the relative phase of the evaluation microphones with and without a person in the driver seat. A positive difference indicates that the relative phase shift is worse with a person in the driver seat. Below 130 Hz, the difference in relative phase is small. However, above 130 Hz, a person in the driver seat significantly increases the relative phase between the evaluation microphones.

MIMO or decentralized RCAC with multiple microphones and speakers to minimize the noise at multiple locations. In addition, optimizing microphone placement in order to reduce spatial spillover effects at the evaluation microphones may be advantageous.

REFERENCES

[1] C. R. Fuller and A. H. von Flotow, "Active control of sound and vibration," *IEEE Contr. Sys. Mag.*, vol. 15, no. 6, pp. 9–19, 1995.

[2] P. A. Nelson and S. J. Elliot, *Active Control of Sound*, San Diego, CA: Academic Press, 1992.

[3] S. M. Kuo and D. Morgan, *Active Noise Control Systems: Algorithms and DSP Implementations*, 1st ed. New York, NY: Wiley 1995.

[4] L. A. Sievers and A. H. von Flotow, "Comparison and extensions of control methods for narrow-band disturbance rejection," *IEEE Trans. Sig. Proc.*, vol. 40, no. 10, pp. 2377–2391, 1992.

[5] J. C. Doyle, B. A. Francis, and A.R. Tannenbaum, *Feedback Control Theory*, New York, NY: Macmillan, 1992.

[6] J. Hong and D. S. Bernstein,"Bode integral constraints, colocation, and spillover in active noise and vibration control," *IEEE Trans. Contr. Sys. Tech*, vol. 6, no. 1, pp. 111–120, 1998.

[7] J. S. Freudenberg, C. V. Hollot, R. H. Middleton, and V. Toochinda, "Fundamental design limitations of the general control configuration," *IEEE Trans. Autom. Contr.*, vol. 48, no. 8, pp. 1355–1370, 2003.

[8] P. A. Ioannou and J. Sun, *Robust Adaptive Control*, Prentice Hall, 1996.

[9] K. S. Narendra and A. M. Annaswamy, *Stable Adaptive Systems*, Prentice Hall, 1989

[10] R. Venugopal and D. S. Bernstein, "Adaptive disturbance rejection using ARMARKOV system representations," *IEEE Trans. Contr. Sys. Tech.*, vol. 8, no. 2, pp. 257–269, 2000.

[11] J. B. Hoagg, M. A. Santillo, and D. S. Bernstein, "Discrete-time adaptive command following and disturbance rejection for minimum phase systems with unknown exogenous dynamic," *IEEE Trans. Autom. Contr.*, vol. 53, no. 4, pp. 912–928, 2008.

[12] M. A. Santillo and D. S. Bernstein, "Adaptive control based on retrospective cost optimization," *J. Guid. Contr. Dyn.,* vol. 33, no. 2, pp. 289–304, 2010.

[13] J. B. Hoagg and D. S. Bernstein, "Retrospective cost model reference adaptive control for nonminimum-phase systems," *J. Guid. Contr. Dyn.,* vol. 35, pp. 1767–1786, 2012.

[14] E. D. Sumer and D. S. Bernstein, "Adaptive control of flexible structures with uncertain dynamics and uncertain disturbance spectra," AIAA Guid. Nav. Contr. Conf., Minneapolis, MN, Aug. 2012, AIAA-2012-4437-323.

[15] Y. Rahman, A. Xie, J. B. Hoagg, and D. S. Bernstein, A Tutorial and Overview of Retrospective-Cost-Based Adaptive Control, *Proc. Amer. Contr. Conf.*, Boston, MA, July 2016

[16] E. D. Sumer, J. B. Hoagg, and D. S. Bernstein, "Broadband disturbance rejection using retrospective cost adaptive control," Proc. DSCC, Fort Lauderdale, FL, October 2012, DSCC2012-MOVIC2012-8580, pp. 1-10.